Separation Science and Technology
Publication details, including instructions for authors and subscription information:
http://www.informaworld.com/smpp/title~content=t713708471

Nitrogen Isotope Separation Using Porous Microreticular Cation-Exchange Resin

Masao Ohwaki; Yasuhiko Fujii; Keiichiro Morita; Kunihiko Takeda

To cite this Article Ohwaki, Masao , Fujii, Yasuhiko , Morita, Keiichiro and Takeda, Kunihiko(1998) 'Nitrogen Isotope Separation Using Porous Microreticular Cation-Exchange Resin', Separation Science and Technology, 33: 1, 19 — 31
To link to this Article: DOI: 10.1080/01496399808544753
URL: http://dx.doi.org/10.1080/01496399808544753

SEPARATION SCIENCE AND TECHNOLOGY, 33(1), pp. 19–31, 1998

Nitrogen Isotope Separation Using Porous Microreticular Cation-Exchange Resin

MASAO OHWAKI and YASUHIKO FUJII
RESEARCH LABORATORY FOR NUCLEAR REACTORS
TOKYO INSTITUTE OF TECHNOLOGY
O-OKAYAMA, MEGUROKU, TOKYO 152, JAPAN

KEIICHIRO MORITA and KUNIHIKO TAKEDA
DEPARTMENT OF METALLURGICAL ENGINEERING
SHIBAURA INSTITUTE OF TECHNOLOGY
SHIBAURA, MINATOKU, TOKYO 108, JAPAN

ABSTRACT

A long-distance chromatographic operation was carried out in order to study the isotope accumulation of ^{15}N in the ion-exchange enrichment process by using a porous microreticular cation-exchange resin. Combined bands of ammonium and lithium ions were eluted up to 20 m, and thereafter the ammonium band was eluted up to a total migration distance of 60 m. The constant lengths of the adsorbed bands were maintained throughout the elution, and a sharp boundary at the rear end of the ammonium band was monitored by an electric conductivity meter. The enrichment of both ^{15}N at the rear end of the ammonium band and ^{6}Li at the rear end of the lithium band were confirmed in the experiment. The values of HETP in the system were kept almost constant, 0.49 mm, throughout the migration up to a distance of 60 m. Previously reported works on the same process are analyzed, and an empirical relation for HETP in terms of resin diameter and band velocity has been obtained as HETP $= c(d_p u_B)^{0.84}$.

INTRODUCTION

Ever since Urey first succeeded in concentration of the nitrogen isotope of atomic weight 15 by NH_4^+–NH_3 chemical exchange in 1937 (1), the separation of nitrogen isotopes has been studied by various methods (2).

Chemical-exchange methods of isotope separation, which make use of the equilibrium fractionation of isotopes in two chemical species, have proved to be the most promising methods of separating isotopes of many lighter elements including nitrogen. Ion-exchange isotope separation, which is one of the chemical-exchange methods, is also based on the chemical equilibrium between a stationary phase and a mobile fluid phase. The first experiment on ion-exchange separation of nitrogen isotopes was made by Spedding et al. in 1955 (3). In their experiment the separation factor of the isotopic exchange between the two phases of the dilute ammonium hydroxide solution and the ion-exchange resin (Dowex 50-x12) in ammonium form was measured as 1.0257 ± 0.0002. A continuous operation using a series of ion-exchange resin beds was also described, and a limited number of experiments were conducted on the influence of concentration and flow rate of the eluent on HETP in their work. Later, in the 1980s, Park and his coworkers (4) investigated ^{15}N enrichment by using fine particle ion-exchange resins; resin diameter of 7–10 μm. A rapid exchange rate was observed in this work. In the recent years, Kruglov et al. (5) studied this system using the SMB (simulated moving bed) process for various flow rates under total reflux. In addition, they also carried out a continuous feed operation in order to estimate the separative efficiency of the system. In their results, they put forth some superior features of the process compared with the traditional fractionation processes.

Nowadays, ion-exchange resins have been greatly improved. It appears suitable to again consider the feasibility of ^{15}N enrichment by using porous microreticular ion-exchange resins. In previous work (6), ^{15}N isotope separation using porous microreticular cation-exchange resin of small particle diameter (200–400 mesh) was experimentally studied, and the influence of the eluent concentration on the separation factor and the HETP at a nonsteady state were investigated. HETPs of the process are almost constant in spite of the large difference in the migration velocity according to concentration of the eluent.

In the present work a long-distance operation was carried out with a porous microreticular cation-exchange resin of relatively large particle diameter (80–200 mesh). In this operation, lithium isotope separation was also examined by forming a lithium band between the ammonium and sodium bands. ^{15}N enrichment by ion exchange is attractive, but the energy costs of acid and caustic reagents are decisive factors for production plants. To reduce the cost, it is proposed that ^{7}Li, which is used in PWRs (pressurized water reactors), be produced simultaneously by a ^{15}N enrichment plant.

EXPERIMENTAL

Apparatus

Four ion-exchange glass tube columns (3 cm i.d. and 2 m long) were connected in series. The columns were packed with the sulfonic acid cation-exchange resin TITEC-H2, a porous sulfonic-acid-type resin (80–200 mesh). A pair of platinum electrodes, 1 cm diameter, was set in the bottom of each column for the measurement of electric conductivity to monitor the band boundary. Flexible vinyl-chloride tubing of 2 mm i.d. was used to connect all columns and valves. A floating plate was placed above the resin bed to prevent the eluent from dropping directly into the bed. The temperature was set at 298 K throughout the experiments by circulating the thermostated water through the jackets of the columns.

Experimental Conditions

The cation-exchange resin packed in the columns was preliminarily converted to the H^+ form with 2 M HCl solution. Ammonia solution (1 M) was fed into the column to make an NH_4^+ adsorption band with a length of approximately 140 cm. Then, 1 M LiOH was fed to make a Li^+ adsorption band above the NH_4^+ band. After a 20-cm long Li^+ band had formed, bands of NH_4^+ and Li^+ were eluted down with the 1 M NaOH eluent fed at a rate of 25 cm/h SV (superficial velocity). The effluent which emerged from the column was introduced to the next column by switching the valve at the bottom of the column. The arrangement of the columns for separating isotopes is illustrated in Fig. 1. When the rear boundary of the lithium band moved to the next column (Column 2), the column connection was rearranged by switching the valves set at the top and bottom of the columns. Then the eluent was admitted to Column 2 and the effluent of this column was introduced to Column 3. In addition, a 2 M HCl solution was fed into Column 1 so that the resin bed was regenerated to the H^+ form from the Na^+ form. To confirm the travel of the band boundary, the electric conductivity was monitored. These operations were continued column by column until the migration distance of the band reached 20 m (first stage), where the Li band was taken out of the column system. The elution of ammonium band was continued to 54 m (second stage).

At a migration distance of 54 m, preservation of enrichment during the plant stop was tested. Leaving the ^{15}N-enriched part of the 40-cm band in one column and the preceding ammonium band in the next column, the connection tube was closed with a pinchcock to avoid mixing of the rear enriched part and the front depleted part. Ten days later the operation

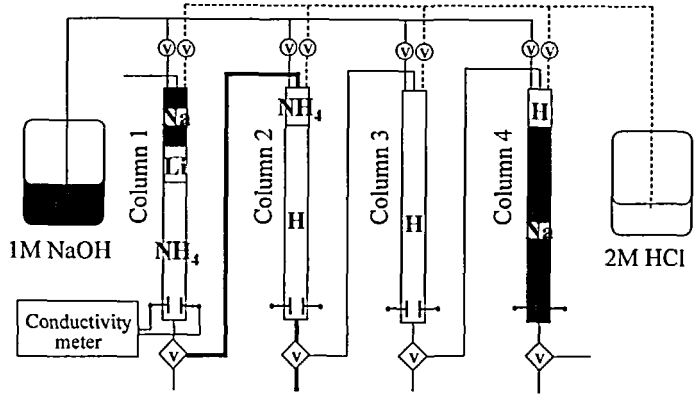

FIG. 1 Chromatographic separation system for ^{15}N enrichment. The thick lines represent the connection at a certain operation time. v = valve

was restarted and continued until the total migration distance was 60 m (third stage).

Sampling and Analysis

A few droplets of the ^{15}N-enriched part were sampled when the migration distance reached 12, 20, 40, 54, and 60 m. For mass spectrometry, the collected samples in the form of NH_{3aq} were neutralized and then converted to N_2 by KBrO. The peaks of $^{14}N^{15}N$ and $^{14}N^{14}N$ of the samples were measured with a double focusing mass spectrometer ESCO EMD-05S. The lithium samples collected at the migration distance of 20 m were measured by a mass spectrometer Varian MAT CH-5 equipped with a thermo-ionization source. The chemical form of lithium was converted to lithium iodide for mass spectrometric analysis.

RESULTS AND DISCUSSION

Chemistry

The separation of nitrogen isotopes by cation-exchange chromatography is based on the isotopic fractionation between NH_3 molecules in the aqueous solution and NH_4^+ ions in the ion-exchange resin:

$$^{14}NH_4^+—R + {}^{15}NH_{3aq} = {}^{15}NH_4^+—R + {}^{14}NH_{3aq} \quad (1)$$

In the first stage of the present system, Na^+ ions in the eluent solution

displace Li^+ ions, and NaOH solution is converted to LiOH in the Li^+ adsorption band due to the large ion-exchange selectivities of Na^+ ions against Li^+ ions:

$$Li^+—R + NaOH \rightarrow Na^+—R + LiOH \quad (2)$$

Then, NH_4^+ ions in the NH_4^+ adsorption band are converted to NH_3 molecules and released from the resin by the LiOH solution at the rear boundary of the band because of the small dissociation in basic solution ($pK_b = 4.76$):

$$NH_4^+—R + LiOH \rightarrow Li^+—R + NH_3 + H_2O \quad (3)$$

Any further chemical reactions and isotopic-exchange reactions taking place in the ammonium adsorption band were described in a previous paper (6).

The following isotopic equilibrium is attained in the lithium band between the resin and solution phases:

$$^6Li^+(H_2O)_3—R + {}^7Li^+(H_2O)_4 = {}^6Li^+(H_2O)_3—R + {}^7Li^+(H_2O)_4 \quad (4)$$

Since hydration of the lithium ion is reduced in the resin phase compared with the solution phase, the heavier isotope tends to be concentrated in the fully hydrated ions in the solution phase. Thus, ^7Li is concentrated at the front boundary.

In previous work (6) the single-stage separation factor was determined using the same type of porous sulfonic acid resin as used in the present work. The single-stage separation factor S is defined by

$$S = \frac{[\overline{^{15}N}][^{14}N]}{[\overline{^{14}N}][^{15}N]} \quad (5)$$

where [ ] denotes the concentration of isotopes in the aqueous phase and [¯] denotes the concentration of isotopes in the resin phase. The single-stage separation factors have been found to decrease slightly with an increase in the eluent concentration. The observed value of S at an eluent concentration of 1 M was 1.0200 ± 0.0020.

Detection of the Band Boundary

In order to conduct a continuous operation successfully, it is necessary to know the location of the band boundaries in a column. In this work the electric conductivity of the eluted solution from the resin bed was measured to monitor the location of the band boundaries. The monitored front and rear boundaries of the ammonium band are shown in Fig. 2,

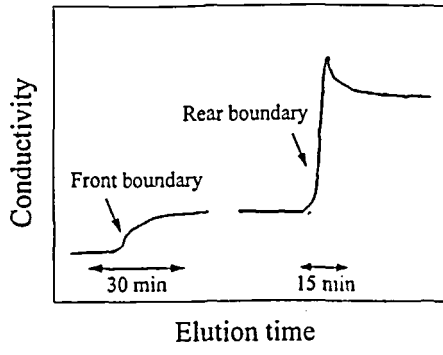

FIG. 2 Monitored conductivity of the ammonium band.

where it is seen that the profile is very sharp at the rear boundary. Since tilted or channeled boundaries give an erroneous isotopic ratio near the band boundaries, as Spedding has stated (3), it is very important to maintain a sharp boundary. The sharp conductivity change monitored in Fig. 2 shows that chemically ideal displacement chromatography is accomplished at the rear of a NH_4^+ band.

Profiles of Isotope Concentration in Bands

The measured ^{15}N isotope concentration profiles at different migration distances are shown in Fig. 3. The migration velocity of a band was kept constant at 2.7 m/d, and the migration was continued for 20 days in the first and second stages. The results apparently show that a steady increase in ^{15}N isotope concentration at the rear end of the band is accomplished with an increase in the migration distance. In the case of the 54-m migration (the end of the second stage), ^{15}N was enriched to 9.3% from its original atomic fraction of 0.365%. On the other hand, the maximum enrichment of ^{15}N was slightly lowered to 8.2% at the migration distance of 60 m. This is due to the interruption of the chromatographic operation for 10 days. Although the accumulation curve was slightly broadened at the migration distance of 60 m, it is shown that the present separation system can be safely stopped for 10 days without serious damage to the enrichment. This suggests that the enriched part can be maintained even if there is an accidental stop in operation.

The enrichment of lithium isotopes is also accomplished in the lithium band which follows the ammonium band. The lithium isotope concentration profile of the rear part of the band at a migration distance of 20 m is

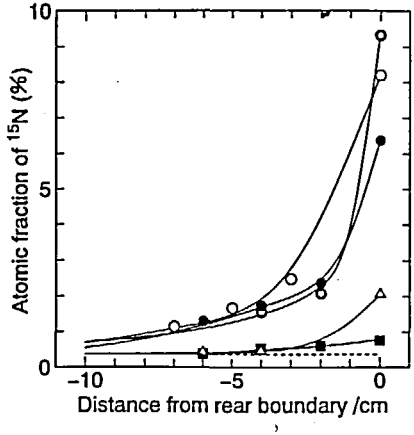

FIG. 3 The measured ^{15}N isotope concentration at the rear boundary. Migration distances: 12 m (■), 20 m (△), 40 m (●), 54 m (○), 60 m (○). The dashed line is the original ^{15}N isotope concentration; $R_0 = 0.00365$.

shown in Fig. 4. The ^{6}Li isotope is enriched at the rear of the band and the ^{7}Li isotope at the front. Since the isotope concentration profile in the figure shows a linear relationship on the semilogarithmic graph without an isotopic plateau region, it is confirmed that the lithium band of 20 cm is already in the steady state by that time. After the steady state, further

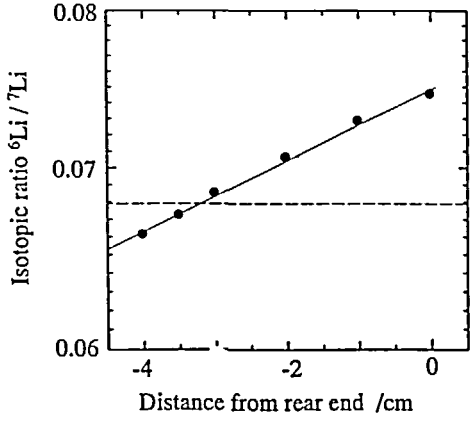

FIG. 4 The measured isotopic ratio in the lithium band at a migration distance of 20 m. The dashed line is the original isotopic ratio; $r_0 = 0.0679$.

enrichment cannot be expected, for then the lithium band was eluted out from the ion-exchange column system.

Since a highly concentrated solution of alkaline was periodically fed into the columns during chromatographic operation, the degradation, or loss, of the ion-exchange resin should be evaluated to estimate the size of the ^{15}N production plant needed. For this purpose, the effluent volume was weighed to calculate the ion-exchange capacity of the resin beds. The determined ion-exchange capacities are plotted against the migration distance in Fig. 5. It is confirmed that the ion-exchange capacity remains constant throughout the chromatographic operation.

HETP

In order to evaluate the efficiency of ^{15}N enrichment in chromatographic migration, HETP (height equivalent to a theoretical plate) is introduced. HETP is usually calculated using the slope of the isotopic distribution curve in the steady-state of isotope separation after a long migration or obtained by a computer calculation fitting based on cascade theory. In previous work, Aida and one of the present authors (Y.F.) (7) proposed the following equation as applicable to nonsteady-state isotope enrichment:

$$H = \frac{\epsilon}{k}\left\{1 + \frac{R_0}{\exp(\epsilon k R_0 L) - 1}\right\} \tag{6}$$

where H is the HETP, ϵ is the separation coefficient, k is the slope defined by following Eq. (7), R_0 is the original isotope atomic fraction, and L is

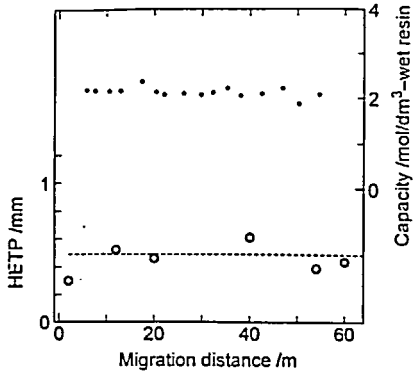

FIG. 5 Observed HETPs and ion-exchange capacity. HETP: (O). Ion-exchange capacity: (●).

the migration length. The value of k is obtained from

$$\ln(r - r_0) = k(L - x) \tag{7}$$

where r is the isotopic ratio (= [^{15}N]/[^{14}N]), and the term $(L - x)$ is the distance of the location x from the rear boundary of which the migration length is L. Equation (7) indicates that plotting $\ln(r - r_0)$ against $(L - x)$ for experimental data yields a linear line with a slope of k. In the present work, Eqs. (6) and (7) are applied to the ^{15}N enrichment system where $R_0 = r_0/(1 + r_0) = 0.00365$ and $\epsilon = 0.0200$. The determined HETP of each migration distance is plotted in Fig. 5. It is seen that the HETP of a single column operation at a migration length of 2 m is somewhat smaller than the other HETPs at longer migrations. This is probably due to the fact that liquid mixing occurs in the dead volume existing between columns when elution is conducted in a multicolumn system. However, it is confirmed in Fig. 5 that the HETPs obtained at a longer migration distance are almost constant (0.49 mm) for migrations up to 60 m.

We have surveyed previously reported ^{15}N ion-exchange enrichment systems, and the HETPs reported by Spedding (3), Park (4), and Kruglov (5), and the calculated HETP based on the data in the work of Urgell (8) are summarized in Table 1 along with the HETPs obtained in the present work and in our previous work (6). Spedding (3), Park (4), and Urgell (8) used gel-type resins; Kruglov (5) used a macroreticular resin; and a highly crosslinked, highly porous microreticular resin was used in our previous work (6). The eluent concentrations were 0.12 and 0.6 M in the experiments by Spedding (3); 0.3 and 0.6 M by Park (4); 0.6 M by Urgell (8); 0.98 M by Kruglov (5); and 0.11, 0.22, 0.53, and 1.14 M in our previous work (6).

The methods of calculating HETP also differed among these studies. In the work of Spedding and Kruglov, HETP were calculated from the slope of the isotopic distribution curve in the steady state of the isotope separation. On the other hand, Park applied computer fitting to the experimental results of nonsteady-state enrichment based on the theory of square cascades with total reflux. For the work of Urgell, the present authors applied slope analysis to the reported enriched isotopic profile. The calculated values given by the computer fitting and our slope analysis on the nonsteady-state experiment agreed well when a comparison was made using the enrichment profile reported by Park (4). HETP is plotted against the product of average resin diameter and band velocity in Fig. 6, where the open and filled symbols show the single column operations and the long distance operations with a multicolumn system, respectively. It is seen in Fig. 6 that there is a linear relationship between ln(HETP) and $\ln(d_p u_B)$, irrespective of the calculation methods. The slope of the

TABLE 1
Details of Operational Parameters and Results

Resin name (x: crosslinking)	Resin structure	Column operation	Average resin diameter (μm)	Band velocity (cm/min)	Concentration of eluent (M)	HETP[a] (cm)	Reference
Dowex 50w-x12	Gel	Multi	126	1.42	0.6	0.155	Spedding (3)
Dowex 50w-x12	Gel	Multi	126	0.28	0.6	0.066	Spedding (3)
Dowex 50w-x12	Gel	Multi	126	0.28	0.12	0.044	Spedding (3)
Dowex 50w-x12	Gel	Multi	126	0.057	0.12	0.017	Spedding (3)
Dowex 50w-x12	Gel	Multi	126	0.36	0.6	0.059	Urgell (8)
Dowex 50w-x12	Gel	Single	126	0.51	0.6	0.071	Park (4)
AG 50w-x12	Gel	Single	126	0.36	0.6	0.047	Park (4)
AG 50w-x12	Gel	Single	56	0.36	0.6	0.0173	Park (4)
Animex A-9	Gel	Single	11.5	0.46	0.6	0.0054	Park (4)
Benson BC-x16	Gel	Single	8.5	0.47	0.6	0.016	Park (4)
Benson BC-x12	Gel	Single	8.5	0.46	0.6	0.0074	Park (4)
Benson BC-x12	Gel	Single	8.5	0.35	0.6	0.0056	Park (4)
Benson BC-x12	Gel	Single	8.5	0.18	0.3	0.0045	Park (4)
Benson BC-x12	Gel	Single	8.5	0.24	0.6	0.0042	Park (4)
KU2-x8	Macroreticular	Multi	700	0.48	0.98	0.70	Kruglov (5)
KU2-x8	Macroreticular	Multi	700	1.83	0.98	0.96	Kruglov (5)
KU2-x8	Macroreticular	Multi	700	2.89	0.98	1.27	Kruglov (5)
KU2-x8	Macroreticular	Multi	700	5.48	0.98	1.70	Kruglov (5)
KU2-x8	Macroreticular	Multi	700	6.97	0.98	2.20	Kruglov (5)
TITEC H1-x30	Microreticular	Single	56	0.35	0.11	0.013	Ohtsuka (6)
TITEC H1-x30	Microreticular	Single	56	0.68	0.22	0.019	Ohtsuka (6)
TITEC H1-x30	Microreticular	Single	56	0.97	0.53	0.015	Ohtsuka (6)
TITEC H1-x30	Microreticular	Single	56	1.70	1.14	0.014	Ohtsuka (6)
TITEC H2-x22	Microreticular	Single	126	0.19	1.0	0.030	Present work
TITEC H2-x22	Microreticular	Multi	126	0.19	1.0	0.049	Present work

[a] HETP analysis: In References 3 and 5, steady-state experiment; in Reference 4, nonsteady-state computer fitting; in References 6 and 8 and the present work, nonsteady-state analytical model.

line shown Fig. 6 is 0.84, which means that the empirical relationship given for most resins tested is

$$\text{HETP} = c(d_p u_B)^{0.84} \tag{8}$$

where c is a constant. On the other hand, the HETPs obtained in our previous work using a porous microreticular resin appear to be somewhat lower than the line in Fig. 6.

In general, HETP depends on the such characteristics of a resin as diameter, crosslinking, etc., as well as the eluent concentration and the band velocity. In order to compare experimental data on the basis of some

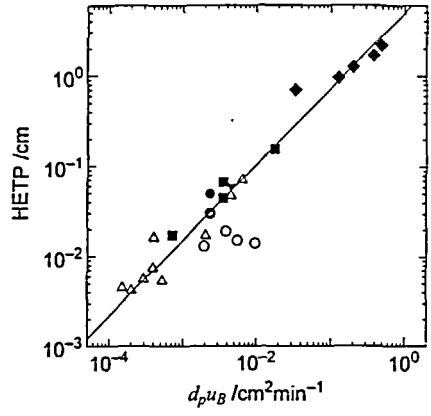

FIG. 6 Effect of band velocity and resin diameter on HETP. HETPs of gel type resins: (■) Spedding et al. (3), (△) Park et al. (4), (▼) Urgell et al. (8). HETPs of macroreticular resin: (◆) Kruglov et al. (5). HETPs of microreticular resins: (○, ●) the present work, (○) our previous work (6). Open symbols: single column operations. Solid symbols: multicolumn operations.

common yardstick, dimensionless parameters (called the reduced plate height h and the reduced velocity v) were introduced by Giddings (9). These are defined by

$$h = \mathrm{HETP}/d_p \tag{9}$$

$$v = d_p u_B / D_m \tag{10}$$

where d_p is the mean diameter of a resin, u_B is the band velocity, and D_m is the diffusion coefficient of NH_4^+ ions in the mobile phase: 1×10^{-5} cm^2/s. The reduced plate height is regarded as a plate height scaled to the particle diameter, and the reduced velocity as the rate of flow compared to the rate of diffusion over a particle. The reduced plate height is plotted against the reduced velocity in Fig. 7. The linear relationship between ln h and ln v is also confirmed in Fig. 7 except for the data obtained by using resin diameters of 8.5 and 11.5 μm. The slope of the line shown in Fig. 7 is 0.43, and the empirical relation obtained is

$$h = dv^{0.43} \tag{11}$$

where d is a constant. In Fig. 7, however, the observed h's of small particle resins (8.5 and 11.5 μm) appear to be higher than the line for other resins. This is probably due to the fact that the homogeneity of the packing was

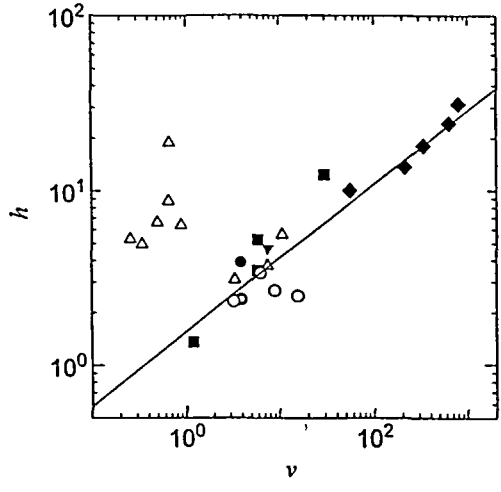

FIG. 7 Plots of reduced plate height vs reduced velocity. Symbols are same as those used in Fig. 6.

reduced when the resin size was decreased because of the *bridging effect* (9). Further studies on porous microreticular resins will provide more information on the influences of flow rate and resin size on the productivity of ^{15}N enrichment by using cation-exchange resin.

CONCLUSIONS

Nitrogen isotope separation was carried out by means of a circuit for continuous displacement chromatography using a porous microreticular cation-exchange resin. The steady increase in the enrichment in atomic fraction of ^{15}N was confirmed at the rear end of an ammonium band. ^{15}N was enriched to 9.3% from its original atomic fraction of 0.365% at a migration distance of 54 m. In this operation, simultaneous enrichment of lithium isotopes was also accomplished by introducing a lithium adsorption band following an ammonium ion band. The ion-exchange capacity was kept constant throughout the chromatographic operation, and a constant value of 0.49 mm was obtained for the HETP of nitrogen isotope separation in the 1–60 m range of migration distances operating at a band velocity of 2.7 m/d. Previously reported ^{15}N ion-exchange enrichment system are surveyed, and an empirical relation for HETP has been obtained [HETP $= c(d_p u_B)^{0.84}$] for most of the resins tested.

ACKNOWLEDGMENTS

The authors acknowledge the kind advice and cooperation of Dr. M. Nomura and Prof. I. Okada, Tokyo Institute of Technology. The present work was financially supported by a Granti-in-Aid of the Ministry of Education, Science and Culture of Japan (Project 07558280) and Power Reactor and Nuclear Fuel Development Corporation.

REFERENCES

1. H. C. Urey, J. R. Huffman, H. G. Thode, and M. Fox, *J. Chem. Phys.*, *5*, 856 (1937).
2. H. G. Spicer, "Proceedings of the International Symposium on Isotope Separation and Chemical Exchange Uranium Enrichment," in Y. Fujii, T. Ishida, and K. Takeuchi (Eds.), *Bull. Res. Lab. Nucl. React., Tokyo Inst. Technol., Special Issue 1*, 91 (1992).
3. F. H. Spedding, J. E. Powell, and H. J. Svec, *J. Am. Chem. Soc.*, *77*, 6125 (1955).
4. W. K. Park and E. D. Michaels, *Sep. Sci. Technol.*, *23*, 1875 (1988).
5. A. V. Kruglov, B. M. Andreev, and Y. E. Pojidaev, *Ibid.*, *31*, 471 (1996).
6. H. Ohtsuka, M. Ohwaki, M. Nomura, M. Okamoto, and Y. Fujii, *J. Nucl. Sci. Technol.*, *32*, 1001 (1995).
7. Y. Fujii, M. Aida, M. Okamoto, and T. Oi, *Sep. Sci. Technol.*, *20*, 377 (1985).
8. M. M. Urgell, J. Iglesias, J. Casas, J. M. Saviron, and M. Quintanilla, *Third United Nations International Conference on the Peaceful Uses of Atomic Energy*, May 1964, A/CONF. 28/P/491.
9. J. C. Giddings, *Dynamics of Chromatography, Part 1*, Dekker, New York, NY, 1965.

Received by editor December 2, 1996
Revision received May 1997